Properties of GaN/ScN and InN/ScN superlattices from first principles

V. Ranjan, S. Bin-Omran, David Sichuga, Robert Sean Nichols, and L. Bellaiche
Physics Department, University of Arkansas, Fayetteville, Arkansas 72701, USA

Ahmad Alsaad
Jordan University of Science & Technology, Department of Physical Sciences, P.O Box 3030, Irbid, Jordan
(Received 27 April 2005; published 4 August 2005)

First-principles calculations have been carried out to reveal structural, electromechanical, electronic, and lattice dynamical properties of GaN/ScN and InN/ScN superlattices—made by alternating *hexagonal* layers of GaN, or InN, with *hexagonal* layers of ScN—for different periods and overall compositions. These nitride systems belong to two different structural classes (having different coordination number), depending on the overall composition. For Sc compositions larger than 50%, each atom has nearly five nearest neighbors. On the other hand, Sc-deficient superlattices adopt a ground state that is nearly fourfold coordinated. This change of structure, and the change in composition or period within the same structure, considerably affect the piezoelectric response, the electronic band gap in magnitude as well as in character (indirect versus direct), and the phonon spectra. We also discussed the relevance of some of these predictions for designing future technological applications.

DOI: 10.1103/PhysRevB.72.085315 PACS number(s): 71.20.Nr, 61.66.Dk, 77.65.−j, 63.20.Dj

I. INTRODUCTION

Gallium nitride and indium nitride have been extensively studied in the last ten years for fundamental and technological reasons, as well as for the differences they exhibit with respect to more conventional III-V semiconductors (such as GaAs, InAs, or AlAs). For instance, the ground state of both GaN and InN is the so-called wurtzite structure—which belongs to the hexagonal symmetry class, is polar and four-times coordinated—that differs from the cubic and nonpolar zinc-blende phase that "usual" III-V semiconductors adopt. Nitrogen is also known to form rather short bonds with Ga or In (e.g., the length of these bonds in GaN and InN is about 80% of those occurring in GaAs and InAs, respectively), which results in exceptionally small atomic volumes in these nitride semiconductor compounds. Consequently, they exhibit a large magnitude of the forbidden gap (e.g., $E_g > 3$ eV in GaN), a considerable hardness, and high thermal conductivity. Some of these properties make the nitrides technologically useful (see Ref. 1 and references therein). As a matter of fact, nitride semiconductors have led to the development of future short-wavelength (green, blue, and ultraviolet) electroluminescence devices.[2–4]

Furthermore, there has also been a long interest in another III-V nitride system, namely ScN. For instance, Travaglini *et al.*[5] performed optical reflectivity measurements on ScN and compared them with the results of the first-principles electronic structure calculations by Monnier *et al.*[6] More recently, first-principles calculations were performed and experiments were carried out[7,8] to determine the band structure of the ScN in its ground-state structure. They predict ScN to be a semiconductor. While most of the previous studies on ScN focused on the ground-state structure (that is, the rock-salt phase[9]), we recently reported the discovery of another stable phase in ScN. Such phase is metastable and is a layered hexagonal (nonpolar) phase that is five-times coordinated,[10] and that we denoted as *h*-ScN (to follow the notation given to a similar phase found in MgO in Ref. 11). Moreover, we further predicted that applying a compressive in-plane strain on *h*-ScN can result in a very high piezoelectric response, as well as a tuning of the electronic band gap in the entire visible range.[12] In other words, it can lead to multifunctionality.

Interestingly, studies dedicated to *solid solutions* made by alloying ScN with GaN or InN are rather scarce,[13–15] while these materials have the potential to yield optimized properties or striking features.[12] For instance, in a recent work we found that superlattices made by alternating *n* layers of ScN with *n* layers of GaN (or InN)—that is, superlattices having an overall Sc concentration of 50%—exhibit a rare phenomenon. More precisely, they undergo an *isostructural* phase transition (from a wurtzite-derived to a *h*-derived phase) when applying a hydrostatic pressure. Such peculiar phase transition was also found to considerably affect piezoelectric, dielectric, and dynamical properties.[15]

The aim of this paper is to predict (and understand) various properties of solid solutions made by alloying hexagonal ScN with hexagonal GaN and InN, *as a function of composition*. More precisely, we have carried first-principles calculations to investigate structural, piezoelectric response, optical and phonon spectrum of (ScN)/(GaN) and (ScN)/(InN) superlattices for different overall compositions and different periods. We focused on short-period superlattices rather than disordered systems for two main reasons. First of all, the accuracy needed to accomplish our aim "forced" us to select first-principles methods as the numerical tool of choice, which forbids us to investigate large systems because their studies would require a large cost in computer time and memory. Second, short-period superlattices have indeed been grown in nitride semiconductors,[16] in general, and in GaN/ScN,[13] in particular.

This paper is organized as follows. Section II indicates the methodology we have used for our calculations. In Sec. III, we show and discuss the properties of these superlattices.

Finally, we present our conclusion in Sec. IV.

II. METHODOLOGY

The systems under investigation in the present work have hexagonal *parent compounds* (e.g., GaN, InN, and/or ScN) with the primitive lattice vectors of the direct Bravais lattice being given by

$$\mathbf{a_1} = a\left(\frac{1}{2}\mathbf{x} - \frac{\sqrt{3}}{2}\mathbf{y}\right),$$

$$\mathbf{a_2} = a\left(\frac{1}{2}\mathbf{x} + \frac{\sqrt{3}}{2}\mathbf{y}\right),$$

$$\mathbf{a_3} = c\mathbf{z}, \tag{1}$$

where a and c are the in-plane and out-of-plane lattice parameters, respectively, and where c/a is the axial ratio. The unit vectors along the Cartesian axes are denoted as **x**, **y**, and **z**. The primitive unit cell for such systems contains four atoms: two N atoms located at $\mathbf{r_1}$ and $\mathbf{r_2}$, and two cations of the same type (e.g., Ga) located at $\mathbf{r_3}$ and $\mathbf{r_4}$, with

$$\mathbf{r_1} = \mathbf{0},$$

$$\mathbf{r_2} = \frac{2}{3}\mathbf{a_1} + \frac{\mathbf{1}}{\mathbf{3}}\mathbf{a_2} + \frac{\mathbf{1}}{\mathbf{2}}\mathbf{a_3},$$

$$\mathbf{r_3} = u\mathbf{a_3},$$

$$\mathbf{r_4} = \frac{2}{3}\mathbf{a_1} + \frac{\mathbf{1}}{\mathbf{3}}\mathbf{a_2} + \left(\frac{\mathbf{1}}{\mathbf{2}} + \mathbf{u}\right)\mathbf{a_3}. \tag{2}$$

Three parameters—a, c/a, and the internal parameter u which determines the relative position of atoms inside the unit cell—are thus needed to fully characterize the binary hexagonal parents. Our previous local-density approximation (LDA) calculations[17,18] predicted that GaN in its equilibrium hexagonal phase has $a=3.1565$ Å(=5.965 Bohr), $c/a=1.631$, and $u=0.376$.[19] The resulting ground-state structure is the so-called wurtzite phase, which is associated with the polar $P6_3mc(C_{6v})$ point group, and which is four-times coordinated. The equilibrium hexagonal phase of InN is also wurtzite, and has 3.5270 Å(=6.665 Bohr), 1.620, 0.378 for a, c/a, and u, respectively, according to our previous first-principles simulations.[19] On the other hand, we recently predicted that the equilibrium value of u and c/a are 0.5 and ≈ 1.207, respectively, for hexagonal ScN [with the in-plane lattice constant being 3.66 Å(=6.916 Bohr)].[10,12] This specific combination of lattice parameters leads to a layered structure—denoted by h-ScN in Refs. 10,12—that is, nearly five-times coordinated and that has a nonpolar $P6_3/mmc(D_{6h})$ space group. Recent experiments support the existence of this unusual h-phase.[14] All our simulated structural parameters for both GaN and InN wurtzite—to be denoted by w-GaN and w-InN, in the following—agree very well with measurements,[20] at the exception of the a in-plane constant (because of the well-known LDA underestimation of about 1–2 % of any lattice parameter), while we are not aware of any growth success and characterization of a pure h-ScN system.

Moreover, the unit cells for the *ternary alloys*, (Sc,Ga)N and (Sc,In)N, under study in the present paper are supercells that consist in stacking different layers along the [0001] direction. For instance, n layers of GaN are stacked on top of m layers of ScN along $\mathbf{a_3}$, resulting in a structure that we denote as either $(\mathrm{GaN})_n/(\mathrm{ScN})_m$ or $n\times m$ superlattice. Note that these ordered structures can be thought of as exhibiting two different kinds of u parameter [see Eq. (2)]: the ones connecting the Ga (respectively, In) and N atoms that are nearest neighbors along the c axis—for which the average over all Ga (respectively, In) atoms is denoted by $\langle u_{\mathrm{GaN}}\rangle$ (respectively, $\langle u_{\mathrm{ScN}}\rangle$)—and the one binding the Sc and its closest N atoms along $\mathbf{a_3}$—for which the average over all Sc atoms is referred to as $\langle u_{\mathrm{ScN}}\rangle$. All the superlattices investigated in this article have a $P3m1(C_{3v})$ group resulting from this stacking. Despite the fact that this space group belongs to the *rhombohedral* symmetry class, we will practically use notations corresponding to a *hexagonal* first-Brillouin zone to index electronic and vibrational properties of (Sc,Ga)N and (Sc,In)N ordered alloys (such index is made possible by the close relationship that rhombohedral and hexagonal symmetry classes share).

Technically, total-energy calculations are performed using the first-principles density-functional theory (DFT) within the LDA,[17,18] and the Vanderbilt ultrasoft pseudopotentials.[21] The valence states for the Sc, Ga, In, and N are taken as $3s^23p^63d^14s^2$, $3d^{10}4s^24p^1$, $4d^{10}5s^25p^1$, and $2s^22p^3$, respectively. We use the Ceperley-Alder[22] exchange-correlation functional as parametrized by Perdew and Zunger.[23] We chose the plane-wave cutoff to be 25 Ry, which leads to converged results of physical properties of interest. We also use a $6\times6\times4$ (respectively, $6\times6\times2$) Monkhorst-Pack (MP) (Ref. 24) k-point grid for Brillouin-zone integration of four (respectively, eight and larger) atoms per unit cell. All the structural degrees of freedom are fully relaxed in every considered structure by following the total-energy and Hellman-Feynman forces (these latter being smaller than 0.051 meV/Å at convergence).

We also compute the spontaneous polarization **P** as a Berry phase of the Bloch states.[25] Piezoelectric coefficients are derived from the knowledge of **P** via:[26]

$$e_{ij} = \frac{1}{2\pi\Omega}\sum_{\alpha} R_{\alpha,i}\frac{d}{d\eta_j}(\Omega\mathbf{G}_\alpha\cdot\mathbf{P}), \tag{3}$$

where $\alpha=1, 2, 3$ denotes the three real-space primitive lattice vectors $\mathbf{R}_\alpha$ (with their component along the i axis being denoted as $R_{\alpha,i}$) and three reciprocal-space primitive lattice vectors $\mathbf{G}_\alpha$. η_j is the macroscopic strain. Ω is the volume of the unit cell and is given by $=\sqrt{3}a^2c/2$, where a and c are the lattice constants. Equation (3) is evaluated by finite differences between two configurations: first that of the ground state, and then for an η_j macroscopic strain relative to this ground state. For this latter configuration the atoms are once again relaxed to respond to the macroscopic strain η_j. In our

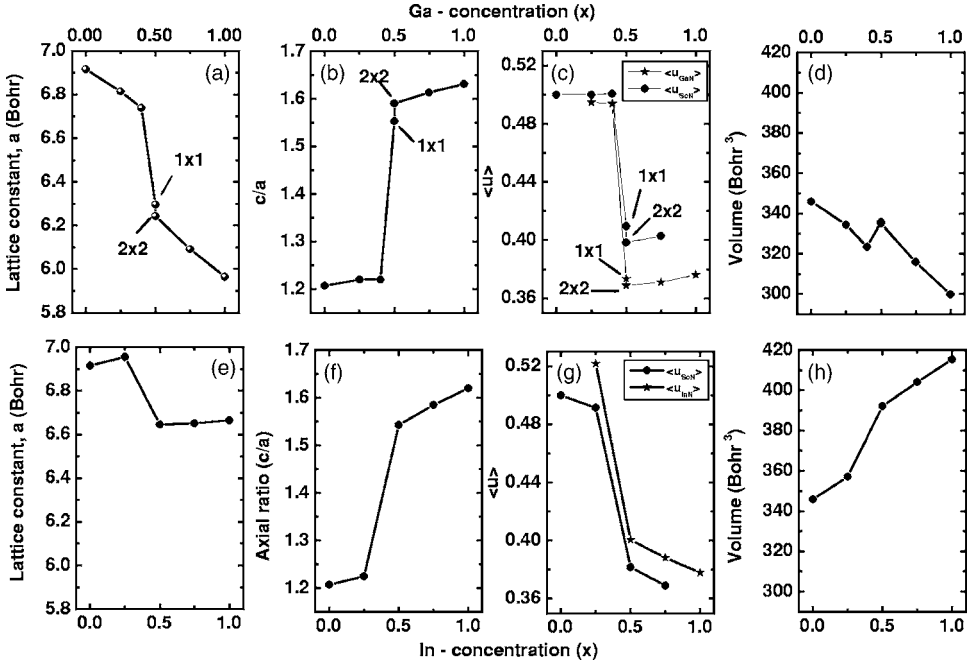

FIG. 1. Variation of the equilibrium in-plane lattice constant (a), the axial ratio (b), the averaged internal parameters (c), and the unit-cell volume (d) as a function of Ga (x) concentration in $(GaN)_n/(ScN)_m$ (e)–(h): same as (a)–(d), but for $(InN)_n/(ScN)_m$. The x composition is given by $x=n/(m+n)$, and the axial ratio shown here corresponds to four atoms per cell. Properties of the parent compounds are also given.

calculations, we have used $\eta_j=\pm 1.5\%$. The final value of e_{ij} is taken as the average of two values obtained for these positive and negative strains.[19] To understand piezoelectric behavior at a microscopic level, one usually decomposes the piezoelectric coefficients into the "clamped-ion" and "internal-strain" contributions:[27,28]

$$e_{33} = e_{33,c} + e_{33,i} \tag{4}$$

The $e_{33,c}$ clamped-ion contribution is calculated using Eq. (3) with the internal coordinates of ions being kept frozen at their unstrained equilibrium positions. The $e_{33,i}$ internal-strain component is solely due to the relaxation of ions when the strain is applied, and is practically computed as the difference between e_{33} and $e_{33,c}$.

Phonon calculations are also performed within the density-functional perturbation theory (DFPT),[29,30] using the ABINIT code[31,32] and the Hatwigsen, Goedecker, and Hutter (HGH) pseudopotentials.[33] Convergence for the ground-state total energy is attained at a plane-wave cutoff of 110 Ry while using HGH pseudopotentials (interestingly, these "hard" HGH pseudopotentials yield equilibrium structural and electronic properties that are remarkably close to those predicted using the "much smoother" Vanderbilt ultrasoft pseudopotentials). The dynamical matrices are calculated on a uniform grid in the unit cell of the reciprocal lattice. The frequency at an arbitrary $\mathbf{q}$ point is obtained by interpolating between the points where a direct calculation of dynamical matrices have already been performed. For all the calculations presented in this work, we found that phonon frequencies are converged for dynamical matrices calculated on $3\times3\times2$ MP mesh. Note that, because of the ionic character of the materials under investigation, the dynamical matrix $D(\mathbf{q})$ displays nonanalytic behavior in the limit $\mathbf{q}\rightarrow 0$.[34] This nonanalyticity, and the related macroscopic electric field associated with the longitudinal optical (LO) mode, is taken into account in the ABINIT code.

III. RESULTS

A. Structural properties

Figures 1(a)–1(d) display the *equilibrium* in-plane lattice constant a, the c/a axial ratio (per four atoms), the averaged internal parameters ($\langle u_{GaN}\rangle$ and $\langle u_{ScN}\rangle$), and the volume per four atoms respectively, as a function of Ga concentration (x) in $(GaN)_n/(ScN)_m$—where $x=n/(m+n)$. Figures 1(e)–1(h) show the same structural information but for the $(InN)_n/(ScN)_m$ structures. The concentration $x=0$ corresponds, of course, to pure ScN whereas $x=1$ corresponds to either w-GaN [in Figs. 1(a)–1(d)] or w-InN [in Figs. 1(e)–1(h)]. The ordered structures considered here are 1×3 (eight atoms per cell and $x=0.25$), 1×1 (four atoms per cell and $x=0.50$) and 3×1 (eight atoms per cell and $x=0.75$) superlattices for both $(GaN)_n/(ScN)_m$ and $(InN)_n/(ScN)_m$ alloys. We also report results for the $(GaN)_2/(ScN)_2$, $(InN)_2/(ScN)_2$ (eight atoms per cell and $x=0.50$) and the computationally demanding $(GaN)_4/(ScN)_6$ (20 atoms per cell and $x=0.40$) solid solutions to better appreciate the role of superlattice *period* and of a *denser* concentration mesh, respectively, on properties of Sc-based and cation-mixed III-V nitride alloys. One can clearly see that $x\simeq0.5$ composition separates two distinct compositional behaviors of the structural parameters in both ScN/GaN and ScN/InN $n\times m$ superlattices. For instance, for $x<0.5$, the axial ratio and the internal parameters are all relatively close to those of h-ScN. The resulting ordered structures are therefore nearly five-times coordinated and will be referred to as "h-derived" in the following. On the other hand, for $x>0.5$, the axial ratio c/a and the internal parameters ($\langle u_{ScN}\rangle$, $\langle u_{GaN}\rangle$, and $\langle u_{InN}\rangle$) become much closer to their value in the ideal wurtzite structure—that are 1.633 for the axial ratio and 0.375 for the internal parameters. These latter structures will be classified as "w derived" and are nearly four-times coordinated. For the intermediate case $x=0.5$, the 1×1 superlat-

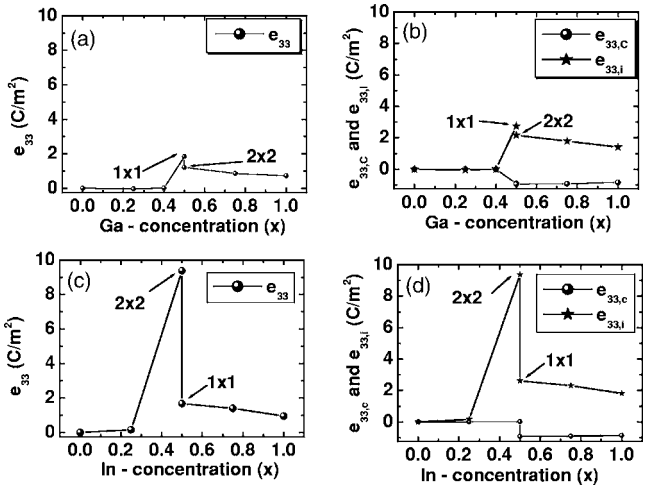

FIG. 2. Piezoelectric coefficient e_{33} as a function of Ga (a) concentration in $(GaN)_n/(ScN)_m$ systems. The clamped-ion ($e_{33,c}$) and internal-strain ($e_{33,i}$) contributions to the the piezoelectric coefficient (e_{33}) are depicted in (b) of the figure. (c) and (d) depict the same as (a) and (b), but for $(InN)_n/(ScN)_m$.

tice stabilizes in *w*-derived structures for both GaN/ScN and InN/ScN alloys. On the other hand, the larger 2×2 superlattice (that also has an overall $x=0.5$ concentration) stabilizes in a *w*-derived structure for GaN/ScN vs *h*-derived phase for InN/ScN. Our predictions for the compositional range of the *w*-derived phase for the GaN/ScN superlattices are consistent with the experimental findings[14] that the ground state of (Ga,Sc)N disordered alloys is (i) wurtzitelike for Ga compositions larger than 70%, (ii) nonwurtzitelike for Ga concentrations smaller than 46%, and (iii) very difficult to determine (transitional regime) for x varying in between. On the the other hand, the nonwurtzitelike phase experimentally seen for the random solid solutions is rocksalt rather than *h*-derived, confirming that (i) the ground state of ScN is cubic rather than hexagonal[10] and (ii) the observation of the *h*-derived phases may require the use of growth techniques leading to *metastable* phases. Note also that the *h*-derived phases may be easily detected in GaN/ScN superlattices (which are the studied systems in this paper) rather than in disordered (Ga,Sc)N alloys because the former exhibits full planes of pure GaN—that prefers to crystallize in a hexagonal structure rather than in the rocksalt phase. It is also important to realize that, although Ref. 14 did not detect a *long-ranged h* phase, interpretations of an observed anisotropic expansion of the ScGaN lattice (that becomes more pronounced when increasing the Sc composition within the wurtzitelike phase) in terms of *local* lattice distortion of atomic bonds strongly support the prediction of a (stable) *h* phase in (Sc,Ga)N and pure ScN systems.[14] Figures 1(d) and 1(h) also reveal that, within a given structure (i.e., *w*- or *h*-derived phase) the volume decreases (respectively, increases) with x composition in $(GaN)_n/(ScN)_m$ [respectively, $(InN)_n/(ScN)_m$], indicating that the ionic radius of Sc is larger (respectively, smaller) than that of GaN (respectively, InN). This hierarchy between ionic radii can also be deduced by realizing that $\langle u_{ScN}\rangle$ is larger than $\langle u_{GaN}\rangle$ in $(GaN)_n/(ScN)_m$ alloys [see Fig. 1(c)], while $\langle u_{ScN}\rangle$ is smaller than $\langle u_{InN}\rangle$ in $n\times m$ InN/ScN superlattices [see Fig. 1(g)]. Interestingly, Figs. 1 also tell us that the composition-induced change in volume is mostly accomplished by the sensitive change in the in-plane lattice constant in $(GaN)_n/(ScN)_m$, while being mainly driven by the evolution of the axial ratio in $(InN)_n/(ScN)_m$. The anisotropic lattice expansion, where the in-plane lattice constant increases much more than the axial ratio, as the concentration of Sc increases in $(GaN)_n/(ScN)_m$ alloys, has indeed been observed for wurtzitelike phases.[14] One can further notice that the superlattice *period*, for a fixed composition, noticeably affects properties, as clearly evidenced by the fact that the 1×1 and 2×2 InN/ScN superlattices have different struc-

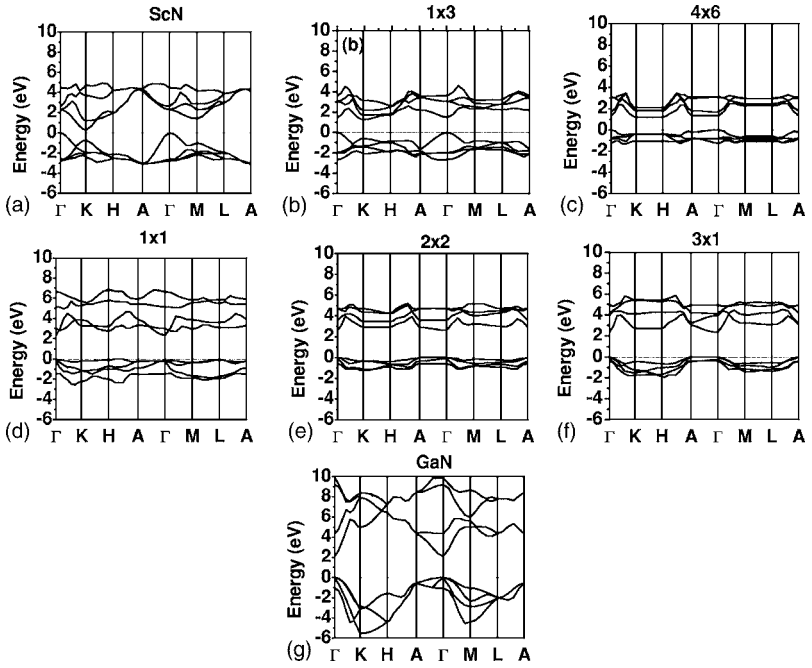

FIG. 3. Electronic band structure of the $(GaN)_n/(ScN)_m$ systems. (a) corresponds to pure ScN, whereas (b)–(g) show the electronic band structure of 1×3 and 4×6, 1×1, 2×2, 3×1, and GaN systems, respectively. The dashed horizontal line shows the zero energy level chosen for the valence band maximum.

TABLE I. The conduction-band energy (CBE) at the Γ point and K point with respect to the valence-band maxima (VBM) for $(GaN)_n/(ScN)_m$ and $(InN)_n/(ScN)_m$ superlattices.

x	$(GaN)_n/(ScN)_m$ CBE (at Γ) (eV)	CBE (at K) (eV)	$(InN)_n/(ScN)_m$ CBE (at Γ) (eV)	CBE (at K) (eV)
0.00	2.289	0.276	2.289	0.276
0.25	1.487	1.242	1.390	1.400
0.40	1.322	1.191		
$0.50(1\times1)$	2.323	3.265	1.600	3.283
$0.50(2\times2)$	2.597	2.907	1.133	1.978
0.75	2.333	2.716	0.69	2.803
1.00	2.093	4.963	−0.200	4.760

tural phases. One can also realize that the $(GaN)_1/(ScN)_1$ and $(GaN)_2/(ScN)_2$, while both adopting a wurtzite-derived structure and having a similar equilibrium volume, exhibit a noticeable difference of about 0.8%, 2.3%, 1.3%, and 2.8% for a, c/a, $\langle u_{GaN}\rangle$, and $\langle u_{ScN}\rangle$, respectively. As we will see later, these differences in structural properties lead to distinct behaviors of other physical quantities.

B. Piezoelectricity

Figures 2(a) and 2(c) display the compositional dependency of the e_{33} piezoelectric coefficient, in $(GaN)_n/(ScN)_m$ and $(InN)_n/(ScN)_m$, respectively. We observe that e_{33} is negligibly small in both kinds of superlattices, when x is smaller than 0.5. This is due to the fact that, for these compositions, the ground state is derived from the "h" phase of ScN, which is a *nonpolar* structure. Conversely, when the Ga or In composition becomes larger than 0.5, the piezoelectricity becomes much larger, as consistent with the fact that the equilibrium structure bears resemblance with the wurtzite phase—which is of *polar* nature. Interestingly, for these latter concentrations, there is a close relationship between e_{33} and the c/a axial ratio: smaller the c/a larger the e_{33}. Consequently, e_{33} decreases when increasing composition above 0.5. Furthermore, $x=0.5$ is the concentration around which both the superlattices GaN/ScN and InN/ScN make a transition from h-derived to w-derived structures. Hence one observes a strong dependency on superlattice period and large values of piezoelectric coefficients around this concentration—especially in the case of $(InN)_2/(ScN)_2$ for which we found (not shown here) two minima (one corresponding to the w-derived phase vs another one associated with a h-derived structure) that are very close in energy. Such large response may be useful to design new piezoelectric devices. Moreover, the decomposition of e_{33} into $e_{33,c}$ and $e_{33,i}$ for GaN/ScN and InN/ScN materials are plotted as a function of composition in Figs. 2(b) and 2(d), respectively. In both kinds of materials, $e_{33,c}$ is mostly a flat (zero) horizontal line for x between 0 and 0.5 and once again a flat (but now negative) horizontal line from 0.5 to 1, whereas $e_{33,i}$ significantly decreases as x changes from 0.5 to 1 (and as the period in GaN/ScN or InN/ScN superlattices having an overall scandium concentration of 50% is increased or decreased, respectively). Hence it is largely the $e_{33,i}$ internal-strain component that is responsible for the trends in e_{33}.

C. Electronic band structure

Figures 3 show the LDA-predicted electronic band structure (neglecting spin-orbit interactions) for all the studied $(GaN)_n/(ScN)_m$ systems, including the parent binary compounds. One can see [Fig. 3(a)] that, as reported earlier,[10] h-ScN is a semiconductor with an LDA *indirect* band gap $\simeq$0.28 eV between a valence-band maximum located at Γ and a conduction-band minimum located at the K point. On the other hand, as it is well known,[20] w-GaN exhibits a direct $(\Gamma\rightarrow\Gamma)$ band gap. Its simulated value is 2.09 eV [see Fig. 3(g)], which is $\simeq$1.4 eV below the measured value of 3.5 eV,[20] as it can be expected from LDA calculations. Interestingly, all the h-derived alloy structures (that is, the 1×3 and 4×6 systems) adopt, as in h-ScN, a valence-band maximum located at Γ and a conduction-band minimum located at the K point (see Table I). Note, however, that the indirect $(\Gamma\rightarrow K)$ band gap becomes much closer to the direct $\Gamma\rightarrow\Gamma$ optical transition in the ordered h-derived solid solutions than in the pure h-ScN (namely, 1.19 vs 1.32, 1.24 vs

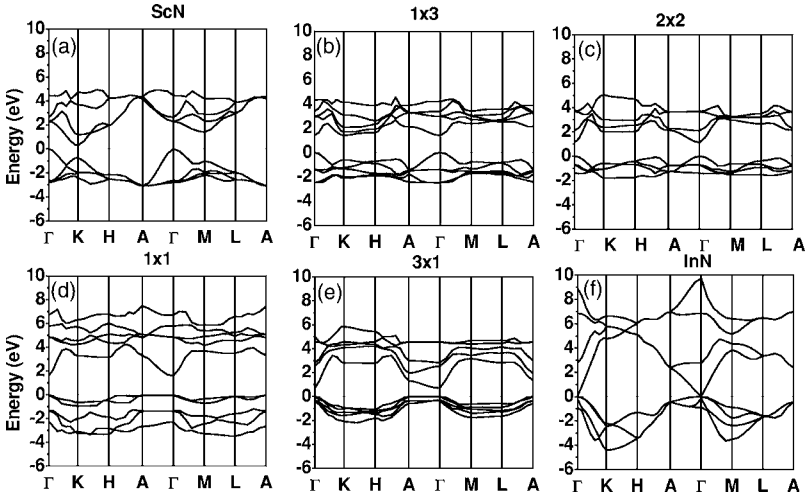

FIG. 4. Electronic band-structure of the $(InN)_n/(ScN)_m$ systems: (a) pure ScN, (b) 1×3, (c) 2×2, (d) 1×1, (e) 3×1, and (f) InN. The trends are described in the text. The dashed horizontal line shows the zero energy level chosen for the valence-band maximum.

TABLE II. Zone-center optical-phonon frequencies for wurtzite GaN and InN in units of cm^{-1}.

		E_2	B_1	A_1(TO)	E_1(TO)	E_2	B_1	A_1(LO)	E_1(LO)
GaN	Experiment[38]	145		533	561	570		735	742
	Bungaro[34]	138	334	550	572	574	690	733	737
	This work	137	337	545	563	572	702	736	732
InN	Experiment[39]					491		590	
	Bungaro[34]	83	225	443	467	483	576	586	595
	This work	85	222	445	467	481	538	588	570

1.49, and 0.28 vs 2.29 eV, according to LDA, in the 4×6 GaN/ScN, 1×3 GaN/ScN, and *h*-ScN systems, respectively). This is consistent with the fact that, based on the electronic structure of the two end members, adding GaN into ScN should favor a direct band gap. Moreover, the *wurtzite-derived* superlattices bear resemblance with *w*-GaN in the sense that their conduction-band minimum is now indexed by the zone-center Γ point and that their Γ-to-Γ transitions are all relatively similar (i.e., 2.32, 2.60, and 2.33 eV for the 1×1, 2×2, and 3×1 GaN/ScN alloys, respectively, to be compared with 2.09 eV for *w*-GaN). On the other hand, one noticeable difference between pure GaN wurtzite and these superlattices having a Ga composition larger than, or equal to, 50% is that the valence band (which is mostly of $2p$-nitrogen character) for the alloys is very flat, especially along the *S* line (connecting *H* and *A*) for the 1×1 structure and along the Γ-to-*A* line for the 2×2 and 3×1 systems. These flatnesses are associated with a large hole effective mass, and should thus lead to a poor hole mobility. Furthermore, the fact that we observe that the 1×1 superstructure shows a distinctly different behavior from the 2×2 ordered alloy demonstrates that this flatness is not "simply" a pure compositional effect: it is also related to chemical ordering (notice, for instance, that the first Brillouin zone of the 2×2 structure is twice as small as that of the 1×1 system, resulting in the folding of some (now interacting) high-symmetry *k* points into other high-symmetry points). It will thus be interesting to measure the flatness of valence bands in *disordered* (Sc,Ga)N alloys, and to compare them with those of our investigated ordered structures. This flatness also leads, in fact, to an *indirect* band gap (with a LDA value of 2.32 eV) for the 1×1 superlattice with the valence-band minimum at a point on the *S* line, being higher by a mere -0.12 eV from the valence band at Γ. Because of this flatness, an indirect ($A\rightarrow\Gamma$) LDA band gap of 2.60 and 2.33 eV is also predicted for the 2×2 and 3×1 systems, respectively, with the difference between the valence-band energy at Γ and the *A* point being a miniscule -10 and -12 meV, respectively (as explained in the caption of Table I).

A similar study of electronic band structure in $(InN)_n/(ScN)_m$ systems is depicted in Figs. 4(a)–4(f). One can clearly see that the *qualitative features* seen in, and discussed above for, $(GaN)_n/(ScN)_m$ also occur in In-mixed alloys. Differences worth mentioning between $(InN)_n/(ScN)_m$ and the $n\times m$ GaN/ScN superlattices are that (a) the 1×3 structure adopts a (barely) direct ($\Gamma\rightarrow\Gamma$) band gap in InN/ScN versus a (slightly) indirect ($\Gamma\rightarrow K$) in GaN/ScN; and (b) the LDA $\Gamma\rightarrow\Gamma$ transition of the 1×1, 2×2, and 3×1 systems are 1.6, 1.133, and 0.69 eV, respectively, in InN/ScN vs 2.32, 2.60, and 2.33 eV in GaN/ScN, because of the smaller band gap of pure GaN with respect to pure InN. Some other energy gaps are also indicated in Table I. It is interesting to note that the Γ-to-Γ band gap of 2×2 InN/ScN is lower than the corresponding one for the 1×1 superlattice, whereas the situation is reversed in the case of GaN/ScN with the band gap being larger for 2×2 superlattices as compared to that of 1×1 superlattices. This may be due to the fact that 2×2 InN/ScN is *h* derived while 2×2 GaN/ScN is *w* derived (while both 1×1 GaN/ScN and InN/ScN are *w* derived). Interestingly, for *x* compositions larger than 0.5 (i.e., in the *w*-derived phases), these In-mixed (respectively, Ga-mixed) superlattices may be useful for designing future devices operating in near infrared to green (respectively, in blue/ultraviolet) color, if one assumes that the LDA conduction energies have to be shifted up by $\simeq0.9$ eV (respectively, 1.4 eV) in wurtzite-derived In-based (respectively, Ga-based) alloys to match the 0.7-eV (respectively, 3.5 eV) experimental values in pure *w*-InN (respectively, *w*-GaN). (Note that 0.7 eV is the band gap recently proposed[35,36] for *w*-InN, which significantly differs from the previously accepted value around 1.8 eV,[37] and may thus still be considered as controversial.) These optical properties, as well as the structural and piezoelectric behaviors revealed and discussed above, makes (Sc,Ga)N and (Sc,In)N solid solutions rather unique and definitely worthy of further theoretical and experimental investigation.

D. Phonon spectra

We now turn our attention to the *lattice dynamics* of the investigated systems. Tables II and III—as well as Figs. 5(a), 5(f), and 6(f)—report our results for *pure* *w*-GaN, *w*-InN,

TABLE III. Predicted zone-center optical-phonon frequencies for hexagonal ScN.

	A_{2u}(TO)	E_{2g}	B_{2g}	B_{2g}	E_{2g}	E_{1u}(TO)	A_{2u}(LO)	E_{1u}(LO)
ScN	269	287	364	508	520	526	640	723

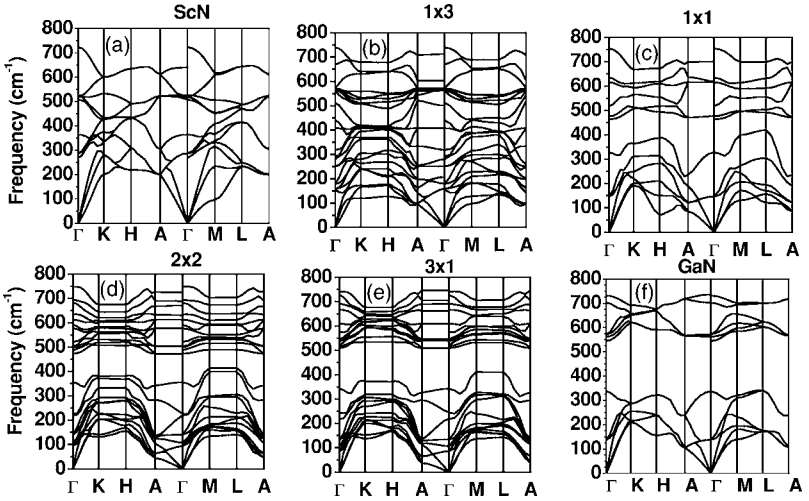

FIG. 5. Phonon spectrum for $(GaN)_n/(ScN)_m$: (a) ScN, (b) 1×3, (c) 1×1, (d) 2×2, (e) 3×1, and (f) GaN. Anisotropy can be observed via the splitting of the highest optical modes along $\Gamma\rightarrow A$ and $\Gamma\rightarrow M$ directions.

and *h*-ScN materials. As stated in Sec. II, *w*-GaN and *w*-InN have C_{6v} symmetry. The phonon modes at Γ point thus have the following decomposition: $2\,A_1+2\,B_1+2\,E_1+2\,E_2$.[34] One A_1 and a doubly degenerate E_1 modes account for the three acoustic phonons. The other A_1 and E_1 modes are both Raman and infrared (IR) active. The E_2 modes are only Raman active while the B_1 modes are silent. As revealed by Table II, there is a very good agreement between our zone-center phonon frequencies and experiments,[38,39] as well as previous first-principles calculations,[34] for both GaN and InN (on the other hand, we are not aware of any previously predicted lattice dynamic studies of *h*-ScN.) This demonstrates that our calculations are highly accurate and that first-principles simulations can nowadays be safely used to predict lattice dynamics.[40] Interestingly, as also mentioned in Sec. II, ScN differs from GaN and InN by its D_{6h} point-group symmetry. Hence we observe in *h*-ScN the following eight-modes decomposition: $2\,B_{2g}+2\,A_{2u}+2\,E_{2g}+2\,E_{1u}$. One A_{2u} and one (doubly degenerate) E_{1u}-mode account for the three acoustic phonons. These are followed by an IR active A_{2u} mode, a doubly degenerate Raman active E_{2g} mode, two silent B_{2g} modes, a doubly degenerate Raman active E_{2g} mode, and finally a doubly degenerate IR active E_{1u} mode for the optical vibrations. (In all there are, of course and as in *w*-GaN and w-InN, 12 normal modes per k point since there are four atoms in the primitive unit cell.) Furthermore and because of the facts that the C_{6v} point group is a subgroup of D_{6h} and that both of these groups have only two-dimensional and one-dimensional irreducible representations, there is a one-to-one relation between the modes for ScN and that of GaN or InN. For instance, the A_{2u} mode of ScN becomes an A_1 mode in GaN and InN. Similarly, B_{2g}, E_{1u}, and E_{2u} in ScN correspond to B_1, E_1, and E_2 in GaN or InN, respectively. It is interesting to realize that the lowest zone-center optical phonon mode in ScN—which is of A_{2u} (TO) symmetry with a 269-cm^{-1} frequency—does not have a one-to-one correspondence with (and is much higher in frequency than) the corresponding ones in GaN or InN—that are of E_2 symmetry with a frequency of 137 and 85 cm^{-1} for GaN and InN, respectively. One can also notice that the difference in frequency between the lowest (respectively, highest) E_2 and B_1 modes is larger in *w*-GaN or *w*-InN than the corresponding difference between the lowest (respectively, highest) E_{2g} and B_{2g} modes in *h*-ScN.

On the other hand, the relative LO-TO splitting, defined as $[\omega(\mathrm{LO})-\omega(\mathrm{TO})]/\omega(\mathrm{TO})$,[34] is larger in *h*-ScN than in both *w*-GaN and *w*-InN. As a matter of fact, this splitting is equal to 0.375 (1.38), 0.31 (0.34), 0.27 (0.28) for the E_1-like

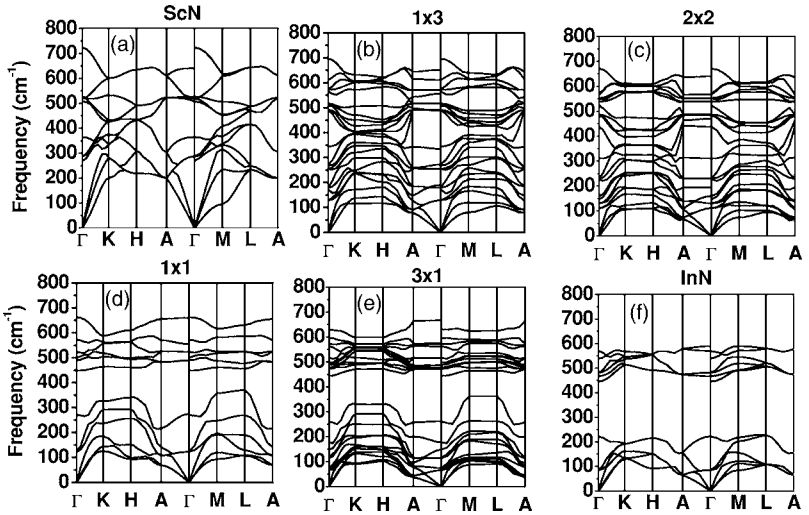

FIG. 6. Phonon spectrum for $(InN)_n/(ScN)_m$: (a) ScN, (b) 1×3, (c) 2×2, (d) 1×1, (e) 3×1, and (f) InN. Anisotropy can be observed the way the highest optical mode splits along $\Gamma\rightarrow A$ and $\Gamma\rightarrow M$ directions.

(*A*-like) modes in *h*-ScN, *w*-GaN, and *w*-InN, respectively. Similarly, the angular dispersion of some optical modes is much more pronounced in *h*-ScN than in *w*-GaN and InN. For instance, $|\{\omega[E_{1u}(\mathrm{LO})]-\omega[A_{2u}(\mathrm{LO})]|/\omega[A_{2u}(\mathrm{LO})]\}$ is equal to 0.13 in *h*-ScN to be compared with $|\{\omega[E_1(\mathrm{LO})]-\omega[A_1(\mathrm{LO})]|/\omega[A_1(\mathrm{LO})]\}$ of 0.01 and 0.03 in *w*-GaN and *w*-InN, respectively. This is due to the fact that *h*-ScN is more anisotropic than *w*-GaN and *w*-InN because of its layered structure (as analogous to the fact that the anisotropy of graphite is very large compared to the diamond phase of carbon[41,42]).

We now discuss the lattice dynamics of some $n\times m$ GaN/ScN and InN/ScN superlattices, that are representative of these alloys, and compare them with those of the parent compounds. More precisely, Figs. 5(b), 5(d), and 5(e) depict the phonon spectra for the 1×3, 2×2, and 3×1 GaN/ScN structures, while Figs. 6(b), 6(c), and 6(e) carry the same information but for the corresponding InN/ScN systems. These superlattices correspond to three different nontransition-metal composition, i.e., $x=0.25$, 0.5, and 0.75, while sharing the same space group $P3m1(C_{3v})$ and the same number of atoms (8) per primitive cell. Therefore they exhibit 24 phonon modes, to be decomposed as $8A_1+8E_1$ with seven A_1 and seven E_1 being both infrared and Raman active. Furthermore, Figs. 5(c) and 6(d) depict the phonon spectra for the 1×1 GaN/ScN and InN/ScN structures, respectively. As the 2×2 structures, the 1×1 superlattices also correspond to an overall Sc composition of 50% and belongs to the same space group $P3m1(C_{3v})$. On the other hand, they have four atoms per unit cell, and thus adopt the following mode decomposition at their zone center: $4A_1+4E_1$. One can clearly see significant differences in the phonon spectrum between the materials exhibiting a *h*-derived phase versus those adopting a wurtzite-derived ground state. In particular, the phonon spectrum of the *h*-derived solid solutions bears resemblance with that of the parent *h*-ScN compound, especially since there is no gap in these spectra. On the other hand, the phonon spectra corresponding to *w*-derived phases looks similar to that of *w*-GaN or *w*-InN, in the sense that gaps have now emerged in these systems. This gap opens up more and more as the Sc concentration decreases. It is within $\simeq$350 and 550, and $\simeq$250 and 450 cm^{-1} for *w*-GaN and *w*-InN, respectively.

Furthermore, the fact that there are now *three* (respectively, *seven*) A_1 and *three* (respectively, *seven*) E_1 modes that all experience a LO-TO splitting in the four atoms per unit cell (respectively, eight atoms) superlattices makes it challenging to quantify LO-TO splitting and uniquely define anisotropy in the alloys. To appreciate this problem, let us first remember that (even infinitesimally) away from Γ along the $\Gamma\rightarrow A$ reciprocal direction, the *z*-polarized A_1 modes "jump" to a higher frequency to form the $A_1(\mathrm{LO})$ modes because of the macroscopic electric field associated with longitudinal optical phonons. Similarly, away from Γ along the $\Gamma\rightarrow M$ reciprocal direction, the *x*-polarized E_1 modes also "jump" to become $E_1(\mathrm{LO})$. In the alloys, because of all these jumps that should be different in magnitude from one A_1 (respectively, E_1) mode to another A_1 (respectively, E_1) mode, assigning the right $A_1(\mathrm{LO})$ [respectively, $E_1(\mathrm{LO})$] mode with its corresponding $A_1(\mathrm{TO})$ [respectively, $E_1(\mathrm{TO})$] becomes a difficult task, which prevents the accurate calculation of LO-TO splitting. On the other hand, it is straightforward to find the frequency of the *highest* $E_1(\mathrm{LO})$ and $A_1(\mathrm{LO})$ modes in the superlattices. We use such frequencies for the computation of the anisotropy of the superlattice, that is the anisotropy is defined as being the absolute value of the relative difference between the *highest* LO E_1 and A_1 modes—as in the pure compounds. Such anisotropy is equal to 0.03 in the (*h*-derived) 1×3 GaN/ScN system, which is considerably smaller than the corresponding value of 0.13 in pure *h*-ScN. This indicates that adding even a small percent of Ga into *h*-ScN reduces quite significantly the anisotropic nature of the material even if the coordination number (that is, nearly 5) remains unchanged. This anisotropy becomes 0.07, 0.03, and 0.01 in the (*w*-derived) 1×1, 2×2, and 1×3 superlattices, that is, it decreases when increasing Ga composition to approach the value of 0.01 in pure *w*-GaN. Adding Sc into the wurtzite phase of GaN thus has a significant effect in increasing the anisotropy of the material even if this material is still nearly four-times coordinated. Similarly, the *h*-derived phases in 1×3 and 2×2 InN/ScN have an anisotropy equal to 0.07 and 0.05, respectively, that is, much smaller than the one $\simeq$0.13 in pure *h*-ScN. Finally, our defined anisotropy is equal to 0.12 and 0.05 in the *w*-derived phases 1×1, and 1×3 InN/ScN superlattices, respectively. In other words, it is decreasing when increasing In composition to approach the value of 0.03 in pure *w*-InN.

Finally, another important finding that can be extracted from Figs. 5 and 6 is that all the systems under study have no lattice instabilities. Therefore we hope that they will successfully be synthesized in a near future.

IV. CONCLUSIONS

In conclusion, we have performed first-principles calculations on $n\times m$ GaN/ScN and InN/ScN superlattices [having the $P3m1(C_{3v})$ symmetry], and compared their results with properties of their GaN, InN, and ScN parent compounds (in their most stable hexagonal form). Superlattices can be divided into two compositionally distinct classes based on their structural properties: for an overall Sc composition larger than 50%, the structural c/a and u parameters of the superlattices are close to that of the hexagonal ScN (that is, $\simeq$1.2 and 0.5, respectively). On the other hand, for an overall Sc composition smaller than 50%, these structural parameters are close to that of the wurtzite structure (that is, $\simeq$1.6 and 0.375, respectively). The transition from hexagonal-derived to the wurtzite-derived class in these ordered alloys is expected at an overall composition of 50%, as emphasized by the fact that the 1×1 and 2×2 InN/ScN systems have different phases. The two different classes are also found to have rather distinct electronic, piezoelectric, and dynamical properties. Some of these properties are technologically promising, e.g., the band gap is predicted to range from near infrared to green for wurtzite-derived InN/ScN superlattices and from near infrared to blue/ultraviolet for GaN/ScN systems in their wurztite-derived phases, when increasing the overall composition of the nontransition-metal cation.

ACKNOWLEDGMENTS

We are grateful for the financial assistance provided by NSF Grant Nos. DMR-0080054 (C-SPIN), DMR-9983678 and DMR-0404335, ONR Grant Nos. N00014-01-0365 (CPD), N00014-01-1-0600 and N00014-04-1-0413, DOE Grant No. DE-FG02-05ER46188, and NATO Grant No. PST.CLG.979025. The authors also acknowledge I. Kornev, H. Fu, I. Naumov, and A.R. Smith for useful discussions. Computational support has been provided by the Center for Piezoelectrics by Design.

[1] V. Ranjan, G. Allan, C. Priester, and C. Delerue, Phys. Rev. B **68**, 115305 (2003).
[2] Shuji Nakamura, Masayuki Senoh, Shin-ichi Nagahama, Naruhito Iwasa, Takao Yamada, Toshio Matsushita, Hiroyuki Kiyoku, and Yasunobu Sugimoto, Jpn. J. Appl. Phys., Part 2 **35**, L74 (1996).
[3] P. Perlin, I. Gorczyca, N. E. Christensen, I. Grzegory, H. Teisseyre, and T. Suski, Phys. Rev. B **45**, 13307 (1992).
[4] N. E. Christensen and I. Gorczyca, Phys. Rev. B **50**, 4397 (1994).
[5] G. Travaglini, F. Marabelli, R. Monnier, E. Kaldis, and P. Wachter, Phys. Rev. B **34**, 3876 (1986).
[6] R. Monnier, J. Rhyner, T. M. Rice, and D. D. Koelling, Phys. Rev. B **31**, R5554 (1985).
[7] D. Gall, M. Stadele, K. Jarrendahl, I. Petrov, P. Desjardins, R. T. Haasch, T.-Y. Lee, and J. E. Greene, Phys. Rev. B **63**, 125119 (2001).
[8] W. R. L. Lambrecht, Phys. Rev. B **62**, 13538 (2000).
[9] N. Takeuchi, Phys. Rev. B **65**, 045204 (2002).
[10] N. Farrer and L. Bellaiche, Phys. Rev. B **66**, 201203(R) (2002).
[11] S. Limpijumnong and Walter R. L. Lambrecht Phys. Rev. B **63**, 104103 (2001).
[12] V. Ranjan, L. Bellaiche, and E. J. Walter, Phys. Rev. Lett. **90**, 257602 (2003).
[13] M. E. Little and M. E. Kordesch, Appl. Phys. Lett. **78**, 2891 (2001).
[14] C. Constantin, H. Al-Brithen, M. B. Haider, D. Ingram, and A. R. Smith, Phys. Rev. B **70**, 193309 (2004).
[15] V. Ranjan, S. Bin-Omran, L. Bellaiche, and Ahmad Alsaad, Phys. Rev. B **71**, 195302 (2005).
[16] P. Ruterana, G. Nouet, W. Van der Stricht, I. Moerman, and L. Considine, Appl. Phys. Lett. **72**, 1742 (1998).
[17] P. Hohenberg and W. Kohn, Phys. Rev. **136**, 864 (1964).
[18] W. Kohn and L. J. Sham, Phys. Rev. **140**, A1133 (1965).
[19] A. Al-Yacoub and L. Bellaiche, Appl. Phys. Lett. **79**, 2166 (2001).
[20] M. Leroux and B. Gil, *Gallium Nitride and Related Semiconductors*, emis Datareviews Series No. 23 (INSPEC, London, United Kingdom, 1999), pp. 45–51.
[21] D. Vanderbilt, Phys. Rev. B **41**, R7892 (1990).
[22] D. M. Ceperley and B. J. Alder, Phys. Rev. Lett. **45**, 566 (1980).
[23] J. P. Perdew and A. Zunger, Phys. Rev. B **23**, 5048 (1981).
[24] H. J. Monkhorst and J. D. Pack, Phys. Rev. B **13**, 5188 (1976).
[25] R. D. King-Smith and D. Vanderbilt, Phys. Rev. B **47**, R1651 (1993).
[26] F. Bernardini, V. Fiorentini, and D. Vanderbilt, Phys. Rev. B **56**, R10024 (1997).
[27] L. Bellaiche and D. Vanderbilt, Phys. Rev. Lett. **83**, 1347 (1999).
[28] L. Bellaiche, Curr. Opin. Solid State Mater. Sci. **6**, 19 (2002).
[29] S. Baroni, P. Giannozzi, and A. Testa, Phys. Rev. Lett. **58**, 1861 (1987).
[30] P. Giannozzi, S. de Gironcoli, P. Pavone, and S. Baroni, Phys. Rev. B **43**, 7231 (1991).
[31] X. Gonze, X. Gonze, J.-M. Beuken, R. Caracas, F. Detraux, M. Fuchs, G.-M. Rignanese, L. Sindic, M. Verstraete, G. Zerah, F. Jollet, M. Torrent, A. Roy, M. Mikami, Ph. Ghosez, J.-Y. Raty, and D. C. Allan, Comput. Mater. Sci. **25**, 478 (2002).
[32] The ABINIT code is a common project of the Universit Catholique de Louvain, Corning Incorporated, and other contributors (URL http://www.abinit.org).
[33] C. Hartwigsen, S. Goedecker, and J. Hutter, Phys. Rev. B **58**, 3641 (1998).
[34] C. Bungaro, K. Rapcewicz, and J. Bernholc, Phys. Rev. B **61**, 6720 (2000).
[35] A. G. Bhuiyan, A. Hashimoto, and A. Yamamoto, J. Appl. Phys. **94**, 2779 (2003).
[36] A. G. Bhuiyan, K. Sugita, K. Kasashima, A. Hashimoto, A. Yamamoto, and V. Yu. Davydov, Appl. Phys. Lett. **83**, 4788 (2003).
[37] T. L. Tansley and C. P. Foley, J. Appl. Phys. **59**, 3241 (1986).
[38] L. Filippidis, H. Siegle, A. Hoffman, C. Thomson, K. Karch, and F. Bechstedt, Phys. Status Solidi B **198**, 621 (1996).
[39] Ming-Chih Lee, Heng-Ching Lin, Yung-Chung Pan, Chen-Ke Shu, Jehn Ou, Wen-Hsiung Chen, and Wei-Kuo Chen, Appl. Phys. Lett. **73**, 2606 (1998).
[40] Note, however, that we predict that the highest optical mode in pure GaN and InN is of A_1(LO) symmetry rather than E_1(LO), which contradicts Refs. 34,38. This discrepancy may be due to the facts that (i) these two modes are very close to each other in frequency and that subtle technical details (such as the choice of pseudopotentials) can affect their hierarchy, and (ii) that the symmetry assigment of the modes, that have been observed by Raman technique, may have been erroneous (Refs. 38,39).
[41] J. C. Phillips, *Bonds and Bands in Semiconductors* (Academic Press, New York and London, 1973).
[42] C. A. Arguello, D. L. Rousseau, and S. P. S. Porto, Phys. Rev. **181**, 1351 (1969).